# PHARMACOPHORE, 3D-QSAR MODELING STUDIES OF HDAC2 LIGANDS AND INSILICO SEARCH FOR NEW HITS

**NARESH KANDAKATLA, GEETHA RAMAKRISHNAN, RAJASEKHAR CHEKKARA**

**Abstract:** Pharmacophore and atom based 3D-QSAR studies were carried out on series of compounds belonging to hydroxamic acid as Histone deacetylase 2 (HDAC2) inhibitors. Based on the ligand based pharmacophore model, 5 point pharmacophore model AADHR - two H-bond acceptors (A), one H-bond donors (D), one hydrophobic group (H) and ring (R) was developed and the generated pharmacophore model was used to derive a predictive atom based 3D-QSAR model for the studied data set of 34 compounds. The developed 3D QSAR model has significant correlation coefficient value ($R^2$ = 0.967) along with high Fisher ration (F = 234.4), low SD value (SD = 0.095) and the model validated by cross validated correlation coefficient ($Q^2$ = 0.602). 3D QSAR results supported by favorable and unfavorable regions of hydrophobic, H bond donors and electron withdrawing groups, these results can be useful for further design of new potent HDAC2 inhibitors. Further pharmacophore model was utilized in virtual screening to identify potential (ZINC4089202, ZINC4000330, ZINC2897245 and ZINC4043342) HDAC2 inhibitors

**Keywords:** Cancer, Hydroxamic acids, HDAC2, Molecular docking, Pharmacophore, QSAR, Virtual screening.

**Introduction:** The chromatic structure of the histone has two forms as acetylated and deacetylated, the equilibrium regulated by histone acetylases (HATs) and histone deacetylases (HDACs) enzymes. Histone binds to negatively charged DNA through positively charged lysine residue N-terminal tails. Lysine residue of the histone N-terminal tail can perform acetylation and deacetylation by histone acetylases and histone deacetylases enzymes [1]-[2]. The equilibrium between HATs and HDACs alter the activity of the residue and affects the chromatin structure and gene activities [3]. Histone deacetylases (HDAC), deacetylases the epsilon-N-acetyl lysine on histone tails and restores the positive charge on lysine residue [4]. HDAC family enzymes are found in plants, fungi, animals, archaebacteria and eubacteria [5]. HDAC family has been classified into four classes based on the homology and yeast proteins. Class I, II and IV operated by Zn dependent mechanism and Class III operated by NAD mechanism. HDAC 1, 2, 3 and 8 belongs to class I and are homologous to yeast enzyme rpd3 and are located in nucleus, HDAC 4, 5, 6, 7, 9 and 10 belong to class II and are homologous to yeast Hda1 and are located in nucleus and cytoplasm, HDAC11 belongs to class IV and Sirtuins (Sirt1-7) belong to class III and are homologous to the yeast silencing protein Sir2 [6]-[7]. Histone deacetylases (HDACs) are consider as viable drug targets for multiple therapeutic applications including various cancers such as colon cancer, lung cancer, cervical carcinoma, breast cancer, kidney/cervix cancer and neurological diseases like Alzheimer's disease, fungal, viral and inflammatory diseases [8]-[10]. The hydroxamic acids as HDAC2 inhibitors are widely reported and first FDA approved hydroxamic acid drug is SAHA (suberoylanilide hydroxamic acid or vorinostat) for treating Cutaneous T-cell Lymphoma [11]-[13]. QSAR studies of HDAC with known inhibitors have been reported early for optimization of HDAC inhibitors as anticancer drugs [14]. Earlier literature on pharmacophore, QSAR of HDAC2 with known benzamide derivatives, benzimidazole and imidazole

derivatives provide information on lead optimization and led compound discovery [15]-[16]. Quantitative structure-activity relationship (QSAR) is computational approach in optimizing the compounds and widely used in drug discovery to reduce the time and cost. The Insilico study with pharmacophore modeling and 3D QSAR were useful in predicting the biological activity of lead compounds.

In the present study Insilico studies on hydroxamic acids were carried out by using pharmacophore modeling, atom based QSAR approaches to design novel potent HDAC2 inhibitors. The best 3D QSAR model utilized for 3D database screening to identify new inhibitors of HDAC2.

**Materials and Methods:**

**Data set:** Data sets of 34 hydroxamic acid derivatives with inhibitory activity against HDAC2 were used for this 3D-QSAR study [17]-[21]. The inhibitory concentration ($IC_{50}$) of these molecules against HDAC2 were converted into corresponding $pIC_{50}$ ($-\log(IC_{50})$) and were used as dependent variables in 3D QSAR calculations (Table 1). The dataset was divided into training and test set. The training set was selected randomly by considering the 80% of training set and 20% of test set. The training set consisted of 28 compounds selected to validate the 3D-QSAR model, other 6 compounds were used as test set.

Table 1: Structures and activity pIC50 of training set and test set compounds 1-34

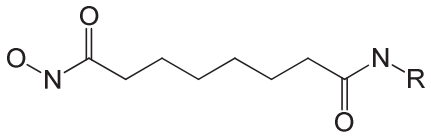


**Common pharmacophore hypothesis (CPH) generation:** Chemical structures of all reported compounds were developed using ISIS draw Ligprep module in Schrodinger and used in ligand preparation to minimize the compound using OPLS_2005 force filed to generate the 3D structure and tatuomers with charge neutralization [22]. This study was performed using the PHASE software for 3D-QSAR pharmacophore development [23]. PHASE utilizes fine-grained conformational sampling and scoring techniques to identify common pharmacophore hypothesis, which convey characteristics of 3D chemical structures that are reported to be critical for binding.

All ligands were imported into PHASE module and conformation generation is an important step in PHASE algorithm. Conformers were generated using Configen model taking distance-dependent dielectric solvent model. Default parameters were used for generation of conformers. About 1000 conformers were generated per structure with 50 step minimization. The minimized conformers were filtered through a relative energy of 10 kcal/mol and minimum atom deviation of 1.00 $A^{o}$ [24]-[25]. 10 kcal/mol values set an energy threshold relative to lower energy conformer, if conformers having higher energy than threshold value are discarded. Thus only lowest non-redundant conformers of ligands were incorporated in the process of pharmacophore development.

The six built pharmacophore features, hydrogen bond acceptor (A), hydrogen bond donor (D), hydrophobic group (H), negatively charged group (N), positively charged group (P) and an aromatic ring (R) were defined by a set of chemical structure patterns as SMART queries and assigned one of three possible geometrics that define the physical characteristics of the site: (1) Point - Site is located on a single atom in SMART query; (2) Vector - Site is located on a single atom in the SMART query and assigned directionality according to one or more vectors originating from the atom; and (3) Group - Site is located at the centre of a group of atoms in the SMART query. For aromatic ring, the site is assigned directionality, defined by a vector that is normal to the plane of the ring. The activity ($pIC_{50}$) of molecules were divided into active (≥

| Compound No | R | $pIC_{50}$ |
|---|---|---|
| 1 (training) | (S)-2-amino-3-(1H-indol-3-yl)-N-(4'-methyl-[1,1'-biphenyl]-2-yl)propanamide | 6.777 |
| 2 (training) | 4'-methyl-[1,1'-biphenyl]-2-amine | 6.612 |
| 3 (training) | 2-methyl-4-(3-nitrophenyl)thiazole | 6.946 |
| 4 (training) | tert-butyl (4'-methyl-[1,1'-biphenyl]-2-yl)carbamate | 7.13 |
| 5 (training) | 3-(2-methylthiazol-4-yl)aniline | 7.568 |
| 6 (test) | 2-amino-N-(4'-methyl-[1,1'-biphenyl]-2-yl)acetamide | 6.438 |
| 7 (training) | ethyl (3-(2-methylthiazol-4-yl)phenyl)carbamate | 7.602 |
| 8 (training) | 2-methyl-4-(2-nitrophenyl)thiazole | 6.536 |
| 9 (test) | tert-butyl (2-(2-methylthiazol-4-yl)phenyl)carbamate | 7.677 |
| 10 (training) | (S)-2-amino-3-(4-hydroxyphenyl)-N-(4'-methyl-[1,1'-biphenyl]-2-yl)propanamide | 6.688 |
| 11 (training) | (S)-2-amino-N-(4'-methyl-[1,1'-biphenyl]-2-yl)-3-phenylpropanamide | 6.806 |
| 12 (test) | 2-methyl-4-phenylthiazole | 7.455 |
| 13 (training) | 2-amino-N-(3-(2-methylthiazol-4-yl)phenyl)acetamide | 7.721 |
| 14 (training) | N-(3-(2-methylthiazol-4-yl)phenyl)acetamide | 8.214 |
| 15 (training) | o-toluidine | 6.995 |
| 16 (training) | 1-phenyl-4-(m-tolyl)-1H-1,2,3-triazole | 7.193 |
| 17 (training) | 1-benzyl-4-(p-tolyl)-1H-1,2,3-triazole | 6.168 |
| 18 (training) | (S)-N-benzyl-2-methyl-3-phenylpropanamide | 6.853 |
| 19 (training) | (S)-2-methyl-N-phenethyl-3-phenylpropanamide | 6.481 |
| 20 (training) | 1-(3-bromophenyl)-2-(4-(p-tolyl)-1H-1,2,3-triazol-1-yl)ethanol | 6.844 |
| 21 (test) | 1-benzyl-5-(m-tolyl)-1H-1,2,3-triazole | 6.95 |
| 22 (training) | 1-(3-bromophenyl)-2-(5-(p-tolyl)-1H-1,2,3-triazol-1-yl)ethanol | 6.665 |
| 23 (training) | 1-benzyl-4-(m-tolyl)-1H-1,2,3-triazole | 7.366 |
| 24 (training) | 1-phenyl-5-(p-tolyl)-1H-1,2,3-triazole | 6.835 |
| 25 (training) | 1-(3-bromophenyl)-2-(4-(m-tolyl)-1H-1,2,3-triazol-1-yl)ethanol | 7.191 |
| 26 (training) | 1-(3-bromophenyl)-2-(5-(m-tolyl)-1H-1,2,3-triazol-1-yl)ethanol | 6.935 |
| 27 (training) | 1-(4-fluorobenzyl)-5-(p-tolyl)-1H-1,2,3-triazole | 7.241 |
| 28 (training) | 1-(4-fluorobenzyl)-4-(m-tolyl)-1H-1,2,3-triazole | 7.111 |
| 29 (training) | 1-phenyl-4-(p-tolyl)-1H-1,2,3-triazole | 7.323 |
| 30 (training) | 1-(4-fluorobenzyl)-4-(p-tolyl)-1H-1,2,3-triazole | 6.531 |
| 31 (test) | 1-(4-fluorobenzyl)-5-(m-tolyl)-1H-1,2,3-triazole | 6.906 |
| 32 (test) | (S)-N-(4'-methyl-[1,1'-biphenyl]-2-yl)pyrrolidine-2-carboxamide | 6.714 |
| 33 (training) | 2-(2-methylthiazol-4-yl)aniline | 7.853 |
| 34 (training) | toluene | 8 |

7) and inactive (≤ 6) setting the maximum and

minimum values in the activity threshold window of PHASE. 15 actives compounds were generated and used for pharmacophore modeling and subsequent scoring.

Common pharmacophore features were identifies from a set of variants – a set of feature type that defines a possible pharmacophore using tree based partition algorithm with maximum tree depth of 3 and the size of pharmacophore box was 1 $A^{o}$ to optimize final common pharmacophore hypotheses (CPHs). The CPHs were examined using scoring function to yield best alignment of the active ligands. The quality of alignment measured by survival score defined as

$S = W_{site}S_{site} + W_{vec}S_{vec} + W_{vol}S_{vol} + W_{sel}S_{sel} + W^{m}_{rew}$

where W and S are weight and score, $S_{site}$ represents alignment score, the RMSD in the site point position; $S_{vec}$ represents vector score, and averages the cosine of the angles formed by corresponding pairs of vector features in aligned structures; $S_{vol}$ represents volume score based on overlap of van der Waals; models of non-hydrogen atoms in each pair of structures; and $S_{sel}$ represents selectivity score, and accounts for what fraction of molecules are likely to match the hypothesis regardless of their activity toward the receptor. $W_{site}$, $W_{vec}$, $W_{vol}$ and $W_{rew}$ have default values of 1.0, where as $W_{sel}$ has a default value of 0.0 was used in hypothesis generation. $W^{m}_{rew}$ represents reward weight defined by $m^{-1}$ where m is the number of actives which match the hypothesis.

**3D-QSAR model building:** PHASE module used in 3D QSAR model for a set of ligands that are aligned to a selected hypothesis. The data set was divided into training (80%) and test set (20%) randomly. Selected hypothesis was used to build the atom based 3D QSAR model. The 3D QSAR model was generated using training set consisting of 28 compounds using grid spacing of 1 Å. The PLS regression method was performed using PHASE module with maximum of N/4 PLS factors (N = number of training set ligands). The generated QSAR model should statistically significant, i.e., it should have good regression value, low RMSE value and should predict the activity of new molecules accurately and identify the active hits from the database. Therefore QSAR model was validated using test set for prediction. The statistical parameters such as $R^2$ (Correlation coefficient), $Q^2$ ($Q^2$ for the predicted activity), Pearson-R (correlation between the predicted and observed activity), SD (Standard deviation), RMSE (Root mean square error), P (Significance level of variance ratio) and F-value were used for the selection of the best QSAR model.

**Database Screening:** The validated pharmacophore hypothesis was subjected to screen against natural database containing 53299 molecules. The main aim of this screening is to find potential lead molecules with increased inhibitory activity against HDAC2 inhibitors. Database hits were ranked in order of their fitness score, phase predicted activity, vector alignment and volume terms. The fitness scoring function is an equally weighted composite of these three terms and ranges from 0 to 3, as implemented in the default database screening in PHASE. The ligands were selected based on the best fitness score and other screening options were kept default.

**Molecular Docking:** The 3D crystal structure of HDAC2 (PDB id: 3MAX) was downloaded from the PDB structural database site (http://www.rcsb.org/pdb). The receptor protein is prepared in discovery studio by removing water molecules and co-crystallized ligand and further applying CHARMm force field to macromolecule 3MAX. The receptor binding sites were searched using flood filling algorithm. The LibDock program implemented in discovery studio was used to define protein site features referred to polar and non polar features, with sphere of 15 $A^{o}$ radius used as the binding area [25]. The Conformations of ligands poses were generated using FAST method and then placed

into the binding area and all are minimized by CHARMm force field. The generated ligands were docked into the defined binding site on the HDAC2 protein. Ligand binding in the receptor cavity was evaluated by scoring function of LibDock score and H-bond interaction.

**Results and Discussion:**

A pharmacophore modeling and 3D QSAR studies were performed on hydroxamic acids to know the effect of spatial arrangement of structural features on HDAC2 inhibition. The pharmacophore model validated against the database to find novel HDAC2 inhibitors.

.

Table 2: Scores of different parameters of the pharmacophore hypotheses using PHASE

| ID | Survival | Site | Vector | Volume | Selectivity | Matches | Activity |
|---|---|---|---|---|---|---|---|
| AADHR | 3.319 | 0.92 | 0.919 | 0.478 | 1.444 | 15 | 7.853 |
| AADDH | 3.318 | 0.89 | 0.946 | 0.483 | 1.642 | 15 | 7.853 |
| AAADH | 3.317 | 0.79 | 0.972 | 0.555 | 1.687 | 15 | 7.568 |

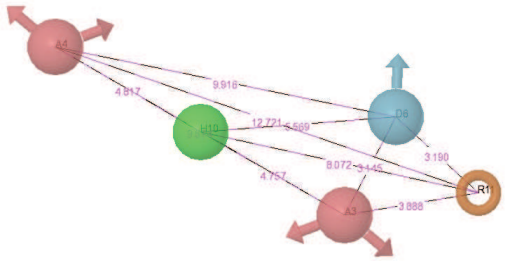


Fig. 1 Generated pharmacophore model AADDH, illustrates two H- bond acceptors (A3, A4; pink), two H-bond donors (D6, D7; blue) and one hydrophobic groups (H10; green) features with distance (A$^o$) between different sites

**Pharmacophore generation:** In pharmacophore model generation, compounds having activity >7 consider as actives and < 6 as inactive compounds. The active compounds contain important structural features for inhibition of HDAC2. 15 compounds represent the active pharmaset were selected for common pharmacophore generation. Tree based partition algorithm requires all 15 compounds should match, 5 featured pharmacophore hypothesis generated from the list of variants. Based on the scoring function three best pharmacophore hypotheses, namely AADHR, AAADH and AADDH, were selected for 3D QSAR model building. The pharmacophore hypotheses AADHR, AAADH and AADDH have survival score of 3.319, 3.318 and 3.317 respectively. The Pharmacophore hypothesis AADHR selected based on the features contains two H-bond acceptors (A), one H-bond donors (D), one hydrophobic group (H) and ring (R) features, the five site pharmacophore model AADHR with inter site distance were shown in fig. 1 The score of the hypotheses are given in Table 2**QSAR Studies:** The three common pharmacophore hypotheses were selected to build the atom based 3D QSAR model. The data set of the compounds was randomly divided into training set (28 compounds) and test set (6 compounds). The activity considered as dependent variables and PHASE descriptors as independent variables for developing 3D QSAR model by PLS regression value. The predictability of the generated 3D QSAR was evaluated by test set compounds. The statistical values $R^2$, SD, F and P were used to evaluate training set and $Q^2$, Pearson -P and RMSE for test set evolution. The QSAR results of three pharmacophore models were given in Table 3. The developed QSAR models predicts high $R^2$ value above 0.9 and F value 234.4, SD less than 0.1 and P value of 6.61E-18 with significant training set of compounds. For selecting best QSAR model not only high $R^2$ value but also predictive ability of the model is considered. The model AADHR has predictive ability $Q^2$ value of 0.6. The statistical values of selected best QSAR model: $R^2$ = 0.967, F = 234.4 and lowest values for SD = 0.095, P = 6.61E-18 for

training set compounds with highest value of $Q^2$ = 0.602, Pearson – P = 0.846 and lowest value of RMSE = 0.266 for test set. The correlation graph between the activity and PHASE predicted activity of training and test set compounds was shown in fig. 2 with best fit. The PHASE predicted and experimental activity of both training and test compounds were given in Table 4.

Table 3: Quantitative Structure Activity Relationship (QSAR) results for the three Common Pharmacophore Hypotheses

| | AADHR | AAADH | AADDH |
|---|---|---|---|
| SD | 0.095 | 0.1566 | 0.1698 |
| $R^2$ | 0.967 | 0.9114 | 0.8824 |
| F | 234.4 | 82.3 | 60.1 |
| P | 6.61E-18 | 9.00E-13 | 2.65E-11 |
| RMSE | 0.2663 | 0.1999 | 0.3796 |
| $Q^2$ | 0.6029 | 0.7428 | 0.4686 |
| Pearson-R | 0.8462 | 0.898 | 0.9407 |

The 3D QSAR model provides the key structural features for ligand interaction with the HDAC2 receptor. The selected AADHR QSAR model is visualized and analyzed with approved drug SAHA using hydrogen bond donors, hydrophobic non-polar, negative and positive ionic, electron withdrawing features.

The results obtained from the 3D QSAR study are useful to find important structural features responsible for biological activity of the ligands. In PHASE generated QSAR model the blue color cubes indicates favorable regions, red color cubes as unfavorable regions for inhibitory activity. Fig. 3a illustrates the presence of blue color cubes at A4 indicates positive potential of H-bond donors and red color cubes at D6 shows negative potential of H-bond donor groups at this position. Fig. 3b demonstrates the presence of blue color cubes at A4 and H10 indicates hydrophobic groups are favorable at these positions, red color group at D6 and H10 shows unfavorable hydrophobic groups at this position and the presence of greater blue color cubes at C-2 position of aromatic ring hypotheses indicates favorable for hydrophobic to enhance

Table 4: Fitness and predictive activity of the training set and test set compounds

| Compound No. | Activity ($pIC_{50}$) | Predicted Activity ($pIC_{50}$) | Residue | Fitness |
|---|---|---|---|---|
| 1 | 6.777 | 6.81 | -0.033 | 2.33 |
| 2 | 6.612 | 6.64 | -0.028 | 2.51 |
| 3 | 6.946 | 7.02 | -0.074 | 2.58 |
| 4 | 7.13 | 7.1 | 0.03 | 1.92 |
| 5 | 7.568 | 7.55 | 0.018 | 3 |
| 6 | 6.438 | 6.64 | -0.202 | 2.25 |
| 7 | 7.602 | 7.49 | 0.112 | 2.5 |
| 8 | 6.536 | 6.73 | -0.194 | 2.49 |
| 9 | 7.677 | 7.3 | 0.377 | 2.66 |
| 10 | 6.688 | 6.76 | -0.072 | 2.41 |
| 11 | 6.806 | 6.79 | 0.016 | 2.42 |
| 12 | 7.455 | 7.65 | -0.195 | 2.15 |
| 13 | 7.721 | 7.79 | -0.069 | 2.8 |
| 14 | 8.214 | 8.12 | 0.094 | 2.08 |
| 15 | 6.995 | 7.14 | -0.145 | 2.56 |
| 16 | 7.193 | 7.17 | 0.023 | 2.54 |
| 17 | 6.168 | 6.04 | 0.128 | 1.91 |
| 18 | 6.853 | 6.82 | 0.033 | 1.91 |
| 19 | 6.481 | 6.46 | 0.021 | 1.96 |
| 20 | 6.844 | 6.87 | -0.026 | 2.24 |
| 21 | 6.95 | 7.21 | -0.26 | 2.02 |
| 22 | 6.665 | 6.51 | 0.155 | 2.27 |
| 23 | 7.366 | 7.45 | -0.084 | 1.97 |
| 24 | 6.835 | 6.8 | 0.035 | 2.01 |
| 25 | 7.191 | 7.26 | -0.069 | 2.45 |
| 26 | 6.935 | 7 | -0.065 | 2.19 |
| 27 | 7.241 | 7.24 | 0.001 | 2.19 |
| 28 | 7.111 | 7.15 | -0.039 | 2.02 |
| 29 | 7.323 | 7.21 | 0.113 | 2.28 |
| 30 | 6.531 | 6.56 | -0.029 | 2.45 |
| 31 | 6.906 | 7.2 | -0.294 | 1.99 |
| 32 | 6.714 | 6.95 | -0.236 | 1.9 |
| 33 | 7.853 | 7.65 | 0.203 | 2.8 |
| 34 | 8 | 8.06 | -0.06 | 2.08 |

the activity of the compounds. Fig. 3c & d illustrates red color cubes at the C-4 position of aromatic ring hypotheses shows unfavorable positive ionic and negative ionic groups. Fig. 3e illustrates the presence of blue color cubes at A4 and C-2 position of aromatic ring hypotheses shows electron withdrawing groups enhances the inhibitory activity and the red color cubes at C-4 position of aromatic ring hypotheses shows electron withdrawing groups decreases the inhibitory activity. Fig. 3f shows combined effects QSAR model. The QSAR model explains the presence of H-bond donors, electron withdrawing groups and hydrophobic groups enhances the inhibitory activity of the compounds. Substitution of these groups at specified positions enhances the activity of the compounds, the H-bond donors at A4, hydrophobic groups at A4, H10 and C-2 position on aromatic ring and electron withdrawing (H - bond acceptors) at C-2 position on aromatic ring are favorable for substitution.

(a)

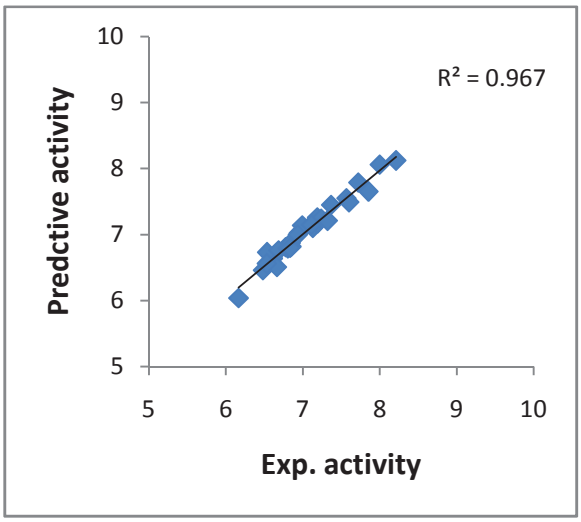


(b)

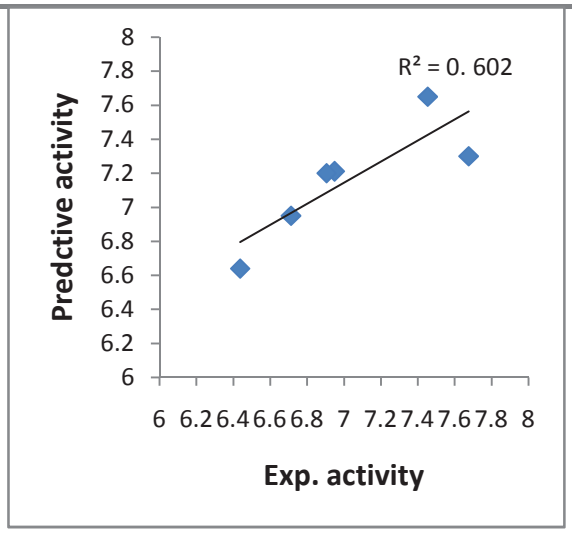


Fig. 2 The scatter plot for the experimental and predictive activity of the (a) training set and (b) test set compounds

(a)

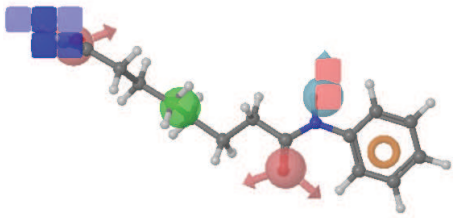

(b)

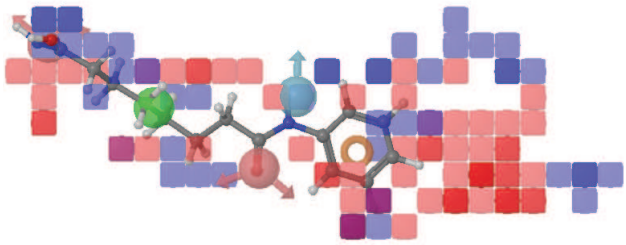

(c)

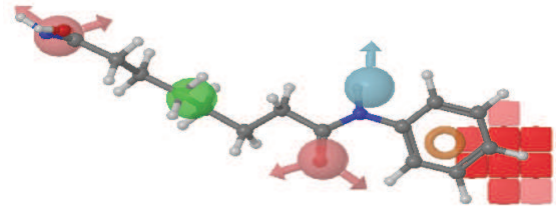

(d)

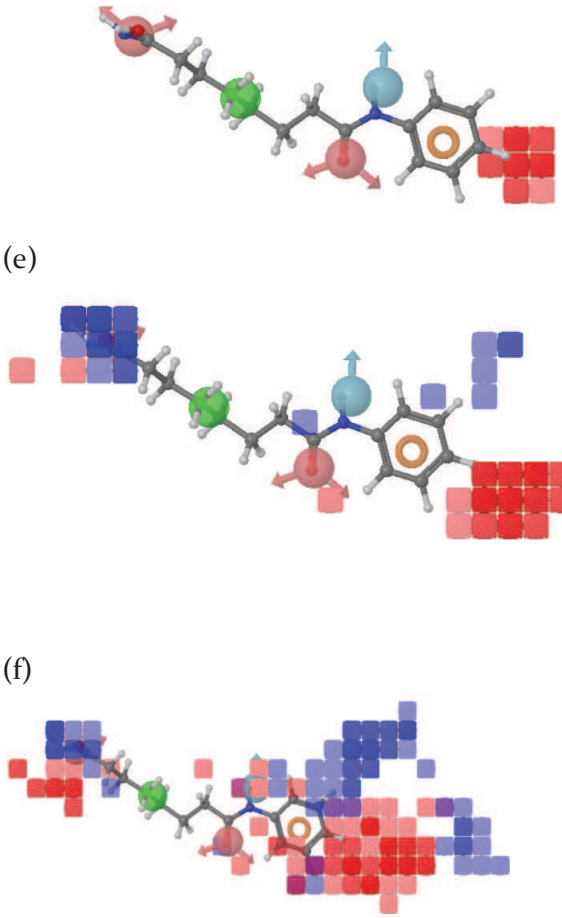

Fig. 3 3D-QSAR visualization for compound 34, (a) H-donor (b) hydrophobic (c) negative ionic (d) positive ionic (e) electron withdrawing (f) combined effect. (Blue cubes favourable influence on activity and red cubes unfavourable influence on activity)

**Database Screening:** The validated AADHR pharmacophore hypothesis was used to search a 3D database for the structures that matches the pharmacophoric features of model. Virtual screening carried out on natural database to find potential lead compounds for HDAC2 inhibition. The lead compounds were selected based on their fitness score and Lipinski's rule of five; compounds have (i) molecular weight less than 500, (ii) less than 5 H-bond donors, (iii) less than 10 H-bond acceptors and (iv) an octanol/water partition coefficient (Log*P*) value less than 5. The final selected lead compounds (571) were subjected to molecular docking studies to find potential lead compounds for HDAC2.

**Molecular Docking:** Molecular docking studies were carried out on lead compounds from natural database screening and optimized compounds from QSAR studies. The HDAC2 protein has 3 chains, chain A is selected for docking studies [27]. The docking score and hydrogen bond interactions were consider for selecting the best pose of the docked compounds. SAHA is chosen as reference compound for comparing the dock score of compounds. The results of docking score and H-bonds are listed in Table 5 and all compounds were ranked by LibDock score. SAHA has 126.37 dock score and 4 hydrogen bond interactions with ARG39 (2), HIS183, GLY305, GLY154 amino acids. The docking pose of top four natural compounds (ZINC4089202, ZINC4000330, ZINC2897245 and ZINC4043342) displayed in fig. 4 ZINC4089202 (N-(2-hydroxy-2-phenylethyl)-2-(4,8,8-trimethyl-2-oxo-2,6,7,8-tetrahydropyrano[3,2-g]chromen-3-yl)acetamide) has the LibDock score of 160.93, five hydrogen bonds with HIS145, GLN265 (2), TYR308, HIS146, GLY154 and also forms pi-pi bonds with LEU144, PHE155 and pi-sigma bonds with ARG39. The docking pose of ZINC4000330 (4,8-dimethyl-2-oxo-3-(3-oxo-3-((pyridin-3-ylmethyl)amino)propyl)-2H-chromen-7-olate) revealed four H bonds with ARG39, CYS156, HIS183, GLY154 and LibDock score of 140.29 and pi-pi bond with ARG39 and pi-sigma with LEU144. For ZINC2897245 (methyl 5-(4-benzamido-3-hydroxytetrahydrothiophen-2-yl)pentanoate) the LibDock score is 138.93, the docked ligand formed four hydrogen bonds with ARG39, HIS145, TYR308 (3), GLY154 and pi-pi bond with PHE155. ZINC4043342 (N-benzyl-6,7-dimethoxy-1-methyl-3,4-dihydroisoquinoline-2(1H)-carboxamide) has LibDock score of 123.98, three H bonds with ARG39, TYR308, GLY154 and pi-pi bonds with PHE155 and ARG39.

The combination of pharmacophore and 3D QSAR study successfully identified key structural features to optimize hydroxamic acids

and the database search provides potent natural compounds to inhibit HDAC2.

(a)

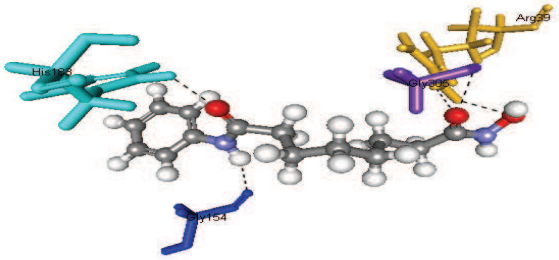


(b)

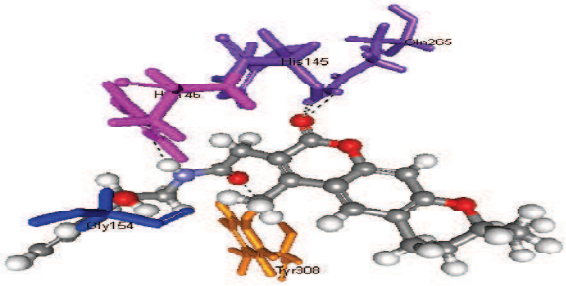


(c)

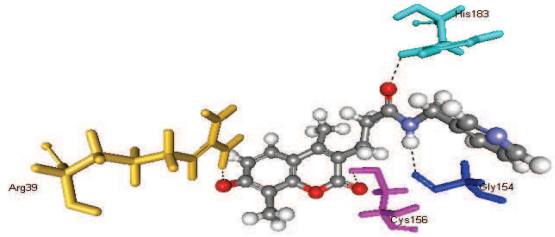


(d)

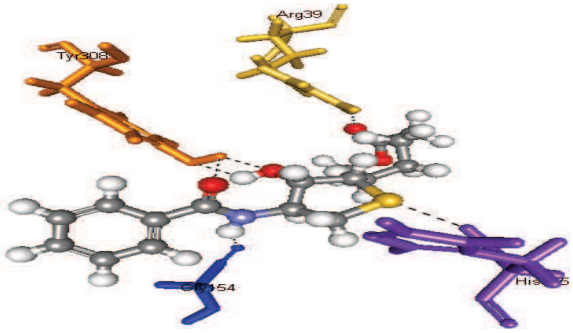


(e)

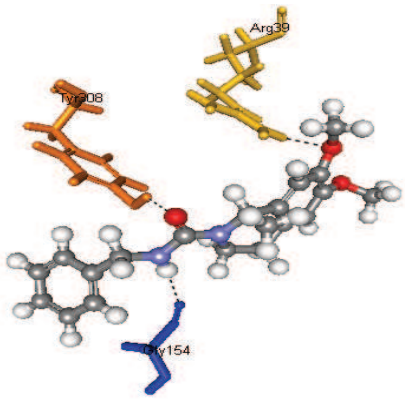


Fig. 4 Docking pose of SAHA and lead compounds (a) SAHA (b) ZINC4089202 (c) ZINC4000330 (d) ZINC2897245 (e) ZINC4043342

Table 5: Docking scores of identified lead compounds and H-bond interactions

| Compound | LibDock Score | H-bonds |
|---|---|---|
| SAHA | 126.37 | ARG39 (2), HIS183, GLY305, GLY154 |
| ZINC4089202 | 160.935 | HIS145, GLN265 (2), TYR308, HIS146, GLY154 |
| ZINC4089775 | 160.181 | GLN265 (2), TYR308, HIS146 |
| ZINC4089507 | 151.481 | GLN265, TYR308 |
| ZINC4089468 | 150.77 | GLN265 (2), GLY306 |
| ZINC8791404 | 148.209 | GLN265 (2), TYR308, HIS146 |
| ZINC4000330 | 140.294 | ARG39, CYS156, HIS183, GLY154 |
| ZINC2897245 | 138.937 | ARG39, HIS145, TYR308 (3), GLY154 |
| ZINC3897389 | 135.987 | ARG39, HIS145, HIS183, GLY154 |
| ZINC4043342 | 123.983 | ARG39, TYR308, GLY154 |

| | | |
|---|---|---|
| ZINC12864369 | 121.889 | ARG39, CYS156 |

**Conclusion:** The present work provides pharmacophore modeling and 3D QSAR studies of some potent hydroxamic acid compounds. Pharmacophore hypothesis of HDAC2 inhibitors were developed using PHASE, these hypotheses were used to build atom based 3D QSAR model. A five point hypothesis AADHR (two H-bond acceptors (A), one H-bond donors (D), one hydrophobic group (H) and ring (R)) provides good 3D QSAR statistical significance and predictive ability. The structure activity relationship of molecules visualized by 3D QSAR model and is utilized in designing better analogues. The 3D QSAR model provides H-bond donors, hydrophobic groups and electron withdrawing groups (H-bond acceptors) were key structural features to design novel compounds to provide better inhibitory activity towards HDAC2 receptor. AADHR pharmacophore hypothesis used as 3D query in searching natural database and subsequent molecular docking studies applied to identify potent HDAC2 inhibitors. Four natural compounds ZINC4089202, ZINC4000330, ZINC2897245 and ZINC4043342 identified as potent HDAC2 inhibitors based on the LibDock score.

**References**


1. C. Monneret, „Histone deacetylase inhibitors“, Eur. J Med Chem, 40, 2005, pp. 1–13.
2. Ruijter, A. J. M. d, Gennip, A. H. v, Caron, H. N, Kemp, S, Kuilenburg, A. B. P. v, “Histone deacetylases (HDACs): characterization of the classical HDAC family”, Biochem J, 370, 2003, pp. 737–749.
3. Jenuwein, T, Allis, C. D., “Translating the histone code”, Science, 293, 2001, pp. 1074-1080.
4. A. Mai, S. Massa, R. Ragno, I. Cerbara, F. Jesacher, P. Loidl, G. Brosch, “3-(4-Aroyl-1-methyl-1H-2-pyrrolyl)-N-hydroxy-2-alkylamides as a new class of synthetic histone deacetylase inhibitors. 1. Design, synthesis, biological evaluation, and binding mode studies performed through three different docking procedures”, J Med Chem, 46, 2003, pp. 512–524.
5. Leipe, D. D, Landsman, D, “Histone deacetylases, acetoin utilization proteins and acetylpolyamine amidohydrolases are members of an ancient protein superfamily”, Nucl Acids Res, 25, 1997, pp. 3693–3697.
6. Anton V. Bieliauskas, Mary Kay H. Pflum., “Isoform-selective histone deacetylas inhibitors”, Chem Soc Rev, 37, 2008, pp. 1402–1413.
7. Sauve AA, Wolberger C, Schramm VL, Boeke JD, “The biochemistry of sirtuin”, Annu Rev Biochem, 75, 2006, pp. 435–465.
8. H. K. Oliver, “HDAC2: a critical factor in health and disease,” Trends in Pharmacological Sciences, 30, 2009, pp. 647-655.
9. K. Mark, A. M. Courtney, M. F. Daniel, M. H. Krista, J. H. Stephen, J. David Sweatt and G. Rumbaugh, “Inhibitors of Class 1 Histone Deacetylases Reverse Contextual Memory Deficits in a Mouse Model of Alzheimer’s Disease“, Neuropsychopharmacology, 35, 2010, pp. 870–880.
10. G.V. Kapustin, G. Fejer, J.L. Gronlund, D.G. McCafferty, E. Seto, F.A. Etzkorn, “Phosphorus-based SAHA analogues as histone deacetylase inhibitors”, Org. Lett, 5, 2003, pp. 3053–3056.
11. Julia M Wagner, Bjorn Hackanson, Michael Lübbert, Manfred Jung, “Histone deacetylase (HDAC) inhibitors in recent clinical trials for cancer therapy”, Clin Epigenet, 1, 2010, pp. 117-136.

12. H. Miles Prince, Mark J Bishton, Simon J Harrison, "Clinical Studies of Histone Deacetylase Inhibitors", Clin Cancer Res, 15, 2009, pp. 3958-3969.
13. Walkinshaw DR, Yang XJ, "Histone deacetylase inhibitors as novel anticancer therapeutics", Curr Oncol 15, 2008, pp. 237-43.
14. Eleni Pontiki, Dimitra Hadjipavlou-Litina, "Histone Deacetylase Inhibitors (HDACIs), Structure Activity Relationships: History and New QSAR Perspectives", Med Res Rev 32, 2012, pp.1-165
15. Naresh Kandakatla, Geetha Ramakrishnan, Vadivelan S, Sarma Jagarlapudi, "QSAR Studies of N-(2-Aminophenyl)-Benzamide derivatives as Histone deacetylase2 Inhibitors", Int J PharmTech Res, 4, 2012, pp. 1110-1121.
16. Xiang Y, Hou Z, Zhang Z, "Pharmacophore and QSAR studies to design novel histone deacetylase inhibitors", Chem Biol Drug Des, 79, 2012, pp. 760-70.
17. Alan P Kozikowski, Yufeng Chen, Arsen M Gaysin, Doris N Savoy, Daniel D Billadeau, Ki Hwan Kim, "Chemistry, biology, and QSAR studies of substituted biaryl hydroxamates and mercaptoacetamides as HDAC inhibitors-nanomolar-potency inhibitors of pancreatic cancer cell growth", Chem Med Chem, 3, 2008 pp. 487-501.
18. Alan P Kozikowski, Yufeng Chen, Rong He, Yihua Chen, Melissa A D'Annibale, Brett Langley, "Studies of benzamide- and thiol-based histone deacetylase inhibitors in models of oxidative-stress-induced neuronal death: identification of some HDAC3-selective inhibitors", Chem Med Chem, 4, 2009, pp. 842-852.
19. Alan P Kozikowski, Kyle V Butler, "Chemical origins of isoform selectivity in histone deacetylase inhibitors", Curr Pharm Des, 14, 2008 pp. 505-528.
20. Alan P Kozikowski, Yufeng Chen, Miriam Lopez-Sanchez, Geoffrey S Dow, Doris N Savoy, Daniel D Billadeau, "A series of potent and selective, triazolylphenyl-based histone deacetylases inhibitors with activity against pancreatic cancer cells and Plasmodium falciparum", J Med Chem 51, 2008, pp. 3437-3448.
21. Bioorg Lori J Pease, Keith B Glaser, Steven K Davidsen, Carol K Wada, Robert B Garland, Michael R Michaelides, Junling Li, Patrick A Marcotte, Jennifer J Bouska, Shannon S Murphy, Robin R Frey, Michael L Curtin, "Trifluoromethyl ketones as inhibitors of histone deacetylase", Med Chem Lett, 12, 2002, pp. 3443-3447.
22. LigPrep, Version 2.3., 2009, Schrodinger, LLC, New York, NY, USA
23. PHASE, version 3.1., 2009, Schrödinger, LLC, New York, NY, USA
24. Dixon SL, Smondyrev AM, Knoll EH, Rao SN, Shaw DE, Friesner RA, "PHASE: a new engine for pharmacophore perception, 3D QSAR model development, and 3D database screening: 1. Methodology and preliminary results", J Comput Aided Mol Des, 20, 2006, pp. 647–671.
25. Dixon SL, Smondyrev AM, Rao SN "PHASE: a novel approach to pharmacophore modeling and 3D database searching", Chem Biol Drug Des, 67, 2006, pp. 370–372.
26. Diller, D.J, Merz, M.L. III, "High Throughput Docking for Library Design and Library Prioritization", Proteins: Structure, Function, and Genetics, 43, 2001, pp. 113-124.
27. Naresh Kandakatla, Geetha Ramakrishnan, "Ligand based Pharmacophore Modeling and Virtual Screening studies for identification of novel inhibitors for HDAC2", Advances in Bioinformatics, 2014, Article ID 812148, 11 pages, http://dx.doi.org/10.1155/2014/812148

* * *

Naresh Kandakatla[1],
Geetha Ramakrishnan [1, *],
Rajasekhar Chekkara[1, 2]
Department of Chemistry, Sathyabama University,
Jeppiaar Nagar, Chennai-600119, India
[2]GVK Biosciences Pvt. Ltd., Plot No: 79, IDA-Mallapur,
Hyderabad-500076, India